Journal of
Nanoscience and Nanotechnology
Vol. 8, 759–763, 2008

Formation of Ge Nanocrystals in Al_2O_3 Matrix

S. Yerci[1,*], M. Kulakci[1], U. Serincan[1], R. Turan[1], M. Shandalov[2], and Y. Golan[2]

[1] Department of Physics, Middle East Technical University, 06531 Ankara, Turkey
[2] Department of Materials Engineering, Ben-Gurion University of the Negev, Beer-Sheva 84105, Israel

Ge nanocrystals were formed in Al_2O_3 matrix by implantation of Ge ions into sapphire (α-Al_2O_3) substrates and subsequent annealing. Diagnostic techniques, Raman spectroscopy, XRD, TEM, EDS, and SAED were employed to monitor and study formation of Ge nanocrystals and their evolution during heat treatments. TEM and EDS analysis revealed the diffusion of Ge ions into the substrate during annealing process. While Ge nanocrystals with mean sizes of 15 nm were observed in the heavily implanted region small nanocrystals with mean sizes of 4 nm were identified underneath this region. Some grains of transition aluminas were formed in the implanted region which was amorphized during the implantation. Extensive stress between the transition aluminas and sapphire matrices and its effects on the matrix were detected. The effect of stress on the Raman and XRD spectra of Ge nanocrystals was discussed.

Keywords: Alumina, Sapphire, Ge, Nanocrystals, Ion implantation, Raman, XRD, TEM.

1. INTRODUCTION

Nanostructured semiconductor materials have received much attention due to their promising applications for optoelectronic/photonic devices[1–3] and non-volatile memory devices.[3,4] These widespread studies have mostly focused on group IV semiconductor nanocrystals, particularly silicon (Si) and germanium (Ge), because of their compatibility with existing silicon based integrated circuit technology. Ge nanocrystals have advantages such as easier modification of the electronic band structure of Ge than that of Si when they are compared basing on the effective masses and energy difference between the indirect and direct gap.[5] In recent years, Ge nanocrystals formed by various methods in SiO_x ($x \leq 2$) matrix (Ge-nc/SiO_x) have been extensively studied. This structure was examined with several analytical techniques to investigate the formation and evolution of the nanocrystals and their behavior (i.e., diffusion) within the matrix.[5,6] Furthermore, prototype devices for electroluminescence and charge capacitance based on Ge-nc/SiO_x structures were produced.[3] The photoluminescence from Ge-nc/SiO_x is considered to originate from Ge-O defect states[7,8] while in some studies it is assumed to result from the quantum confinement of carriers in Ge nanocrystals.[9] SiO_2 films grown on Si substrate is the major dielectric material used to fabricate memory devices in microelectronics because of their superior electrical properties. However, in recent years, high-k dielectrics have been considered to replace SiO_2 for memory applications due to the shrinking dimensions of gate dielectrics. Owing to its high dielectric constant and bandgap similar to SiO_2, Al_2O_3 is a promising candidate as the replacement for SiO_2 in these applications. Thin films of Al_2O_3 can be deposited on Si substrates by various growth techniques used in the integrated circuit technology. Ge nanocrystals can be formed in Al_2O_3 (Ge-nc/Al_2O_3) to form non-volatile, robust, and reliable memory devices with smaller dimensions. Recently, Ge-nc/Al_2O_3 structures were formed using pulsed laser deposition[10] and ion implantation.[11–13] The latter has the advantage of precise control over the dose and location of the implanted ions as well as its compatibility with the present technology. However, it is well known that ion implantation creates defects and can lead to amorphization of the implanted layer which can partially be repaired with subsequent annealing.

In the present study, Ge nanocrystals were formed in α-Al_2O_3 matrix by ion implantation and subsequently annealed at temperatures in the range 500–800 °C. Formation of the nanocrystals was studied with transmission electron microscopy (TEM), Raman spectroscopy, and X-ray diffraction (XRD) measurements. These methods were complementarily employed to observe the evolution of the nanocrystals and the host matrix. While TEM and energy dispersive X-ray spectroscopy (EDS) were used to show the diffusion of the Ge nanocrystals within the matrix, high resolution TEM (HRTEM) was used to determine the approximate sizes of the nanocrystals. Selected

*Author to whom correspondence should be addressed.

1533-4880/2008/8/759/005 doi:10.1166/jnn.2008.A018

area electron diffraction (SAED) was used in order to identify the nanocrystals and different phases of the matrix, and the stress induced deformation of the surface was observed by scanning electron microscopy (SEM).

2. EXPERIMENTAL DETAILS

C-plane oriented α-Al_2O_3 substrates were implanted using 100-keV ^{74}Ge ions at doses of 5×10^{16} and 1×10^{17} Ge ions/cm^2. The samples were subsequently annealed at temperatures ranging between 500 and 800 °C in vacuum for 1 h to induce Ge nanocrystal formation. XRD measurements were conducted with a standard X-ray powder diffractometer, using Cu K_α radiation. Conventional Bragg-Brentano Θ–2Θ scans were employed with scans between 10° and 80° at 0.02° steps. Acquisition time per angular steps of 6 s was used to enhance the signal to noise ratio. Raman measurements were employed in backscattering geometry at room temperature using 632.8 nm (He–Ne laser) as light source in a confocal micro-Raman (HR800, Jobin Yvon), equipped with an Olympus microanalysis system and a peltier cooled CCD camera providing a resolution of ~1 cm^{-1}. Laser power of ~1 mW was used to eliminate nanocrystal formation due to local heating. TEM cross sections were prepared using the wedge technique by mechanical polishing followed by ion milling using a Gatan PIPS ion milling apparatus. TEM images and diffraction patterns were obtained using a JEOL JEM 2010 operating at 200 keV that was equipped with a high resolution pole piece and a Noran energy dispersive spectroscopy detector.

3. RESULTS

3.1. TEM and SEM

TEM micrograph of the sapphire sample implanted with a dose 1×10^{17} Ge ions/cm^2 is shown in Figure 1(a). The projected range of implanted Ge ions is calculated as ~40 nm using a Monte Carlo simulation, TRIM.[14] However, it can be estimated from TEM images as ~60 nm. Furthermore, Ge ions reached up to 200 nm depth were observed using EDS measurements which is not expected from the simulation. We observed similar variation between calculated and measured depth profiles using secondary ion mass spectrometry for sapphire samples implanted with Si ions. The difference between calculated and experimental values can be attributed to the modification of the sapphire matrix and the formation of Ge rich layer during the implantation. A more rigorous calculation taking structural variations during the implantation into account should be employed to remove these discrepancies. The experimental errors in the TEM analysis and the effect of ion channeling during the implantation should also be considered for an exact analysis.

The dark region in Figure 1(a) has the highest concentration of Ge atoms and is most damaged and stressed area. The concentration of Ge atoms decreases with depth after about 60 nm from surface. The dark spots seen at depths between 100–200 nm are well known end-of-range damages resulted from the implantation. The region of approximately first 100 nm and second 100 nm from the surface will be called as region 1 and region 2, respectively.

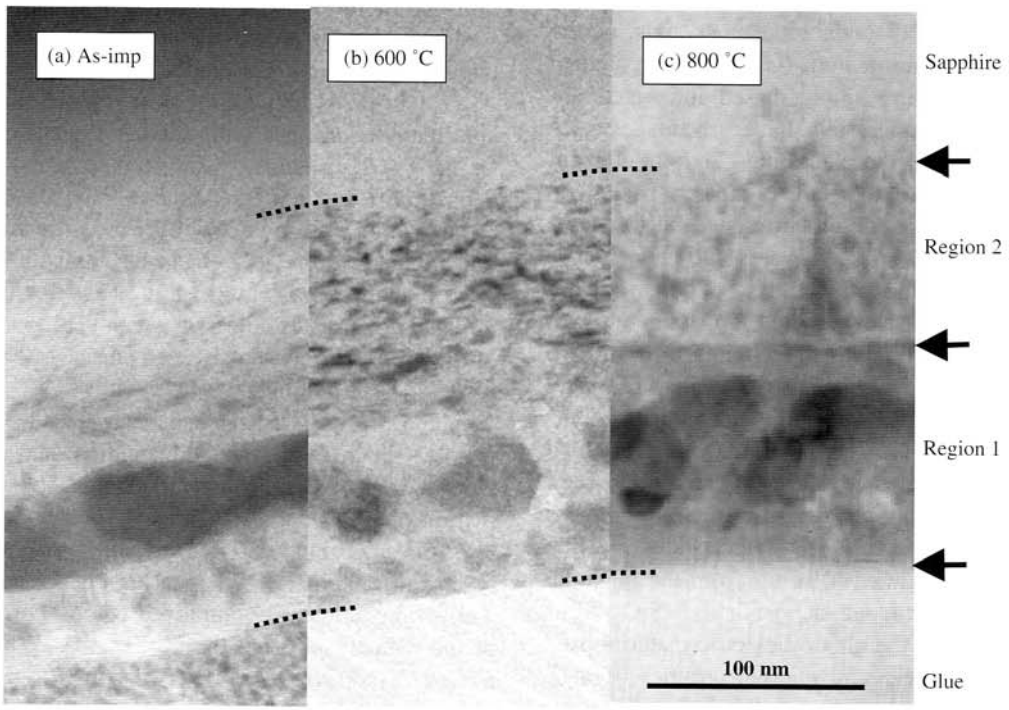

Fig. 1. TEM micrograph of a sample (a) implanted with a dose of 1×10^{17} Ge ions/cm^2 subsequently annealed at (b) 600 °C, and (c) 800 °C. Dashed lines mark the implanted region.

RESEARCH ARTICLE

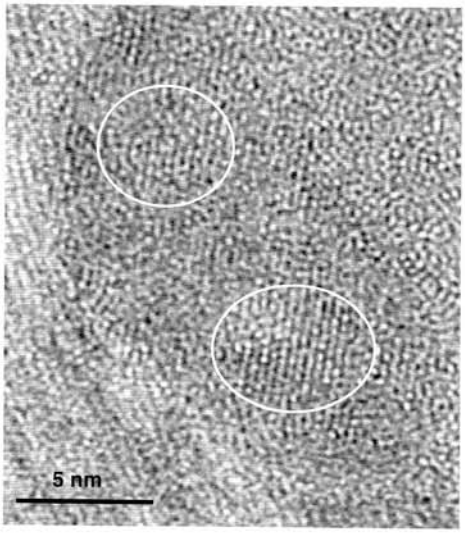

Fig. 2. HRTEM micrograph of the sample implanted with a dose of 1×10^{17} Ge ions/cm^2 and subsequently annealed at 600 °C. Two regions with nanocrystals are marked by circles to guide the eye.

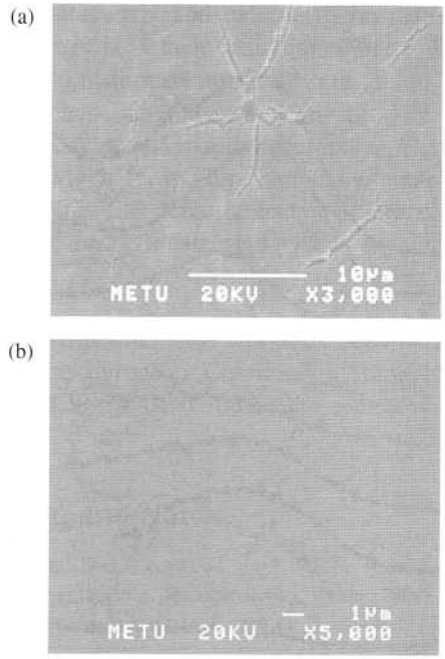

Fig. 3. SEM images of (a) sample implanted with 1×10^{17} Ge ions/cm^2 and subsequently annealed at 600 °C, (b) bulk sapphire reference sample annealed at the same conditions.

The TEM micrograph of the sample implanted with 1×10^{17} Ge ions/cm^2 and subsequently annealed at 600 °C is given in Figure 1(b). It seems that while grains of transition alumina and Ge nanocrystals were formed in region 1, dark spots due to stress field can be observed in region 2. The sizes of the nanocrystals were estimated as ~3 nm using HRTEM (Fig. 2). The phases of the grains could not be identified with SAED, TEM, and XRD; however, one might expect formation of gamma (γ) phase which is most stable at 600 °C.[15] Thus, the defects in sapphire (α-Al_2O_3) for region 2 may be explained in terms of stress between the grains γ-Al_2O_3 and α-Al_2O_3 matrix and the diffusion of Ge ions in sapphire. The effect of stress can be identified on the surface of the wafer in the SEM images of the sample implanted with 1×10^{17} Ge ions/cm^2 and annealed at 600 °C (Fig. 3). Crack formation as a result of extensive stress is clearly seen on the surface of the sample implanted with 1×10^{17} Ge ions/cm^2 and annealed at 600 °C (Fig. 3(a)). The average size of the observed microfractures is of the order of 1 to several μm. An SEM image (Fig. 3(b)) showing bulk sapphire which was annealed at 600 °C under identical conditions is given for comparison.

After an annealing of 800 °C, nanocrystals with average sizes of ~15 and ~4 nm were observed in region 1 and 2, respectively (Fig. 1(c)). After an annealing of 800 °C, nanocrystals with average sizes of ~15 and ~4 nm were observed in region 1 and 2, respectively (Fig. 1(c)). A similar result was previously reported by Xu et al.[13] that Ge nanocrystals with average sizes of 13.1 and 6.2 nm were formed in sapphire samples implanted with a dose of 5×10^{15} Ge ions/cm^2 and an energy of 50 keV after an annealing of 1200 °C. According to Xu et al., the distribution of Ge nanocrystals in sapphire can be fitted by two Gaussians. Although they reported that the formation of Ge nanocrystals in Al_2O_3 starts at higher temperatures than that of in SiO_2, we observed the formation of Ge nanocrystals at temperatures as low as 500 °C using Raman spectroscopy and 600 °C using TEM.[13] The sudden increase in the size of the Ge nanocrystals in region 1 can be due to the coalescence of Ge nanocrystals at 800 °C to form larger nanocrystals. Moreover, it can be seen in Figure 1(c) that sapphire matrix in region 2 starts to recover and a crystalline interface becomes evident between two regions. This band can be due to reformation of α-Al_2O_3 during the annealing.

3.2. XRD

The XRD spectra of implanted samples with doses of 5×10^{16} Ge ions/cm^2 and 1×10^{17} Ge ions/cm^2 and subsequently annealed at temperatures of 700 and 800 °C are given in Figure 4. Sharp peaks at around 20.7° and 37.8° are due to the crystalline bulk substrate. Samples implanted and annealed at lower temperatures (<800 °C) exhibit α-Al_2O_3 peaks only. However, a broad peak (highlighted with #), assigned to Ge nanocrystals with (111) direction, appears at around 27.5° for samples with both implantation doses and same annealing temperature of 800 °C.[10] The broad feature of the peak is due to the decrease in the coherence length (indicating the existence of nanocrystals). The sizes of the nanocrystals were estimated as ~14 nm from XRD peaks using Scherer's formula which is very close to the values estimated from TEM micrographs.[16, 17] On the other hand, the difference between XRD signal observed at 27.5° and the expected

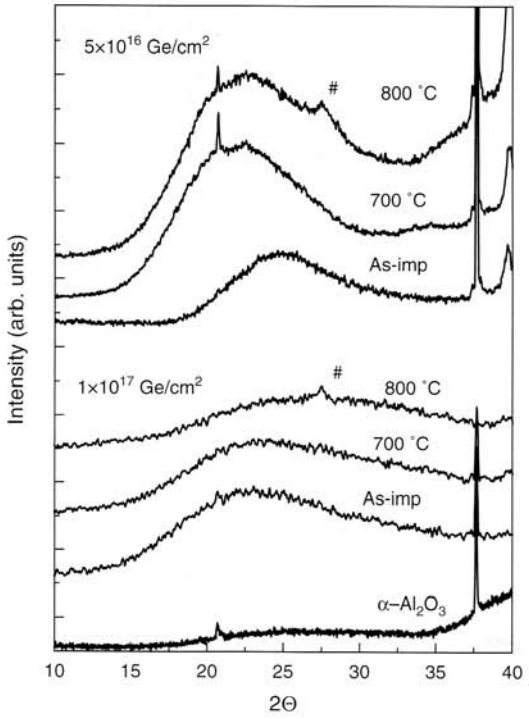

Fig. 4. XRD spectra of the samples implanted with doses of (a) 5×10^{16} Ge ions/cm^2 and (b) 1×10^{17} Ge ions/cm^2 and subsequently annealed at temperatures of 700 and 800 °C. Ge (111) signal is marked with (#).

value of 27.3° for bulk Ge (111) indicates that nanocrystals are under compressive stress. The XRD peak seen at 27.5° resulted from the large nanocrystals formed in region 1 (Fig. 1), created near the projected range of implantation.

3.3. Raman Spectroscopy

Raman spectra of samples implanted with doses of 5×10^{16} Ge ions/cm^2 and 1×10^{17} Ge ions/cm^2 and those of the samples annealed at 600 °C are shown in Figure 5. The observed features of the as-implanted samples correspond to typical amorphous Ge peaks around 170 cm^{-1} and 260 cm^{-1} originating from the LA and TO bands, respectively.[18] The peaks at around 418, 577, and 750 cm^{-1} are due to the crystalline host matrix. Their intensities are higher for the sample implanted with lower dose, indicating the heavier amorphization for the sample implanted with higher dose. Upon annealing at 600 °C, the LA band disappeared almost completely from the spectra and the TO band was shifted towards 300 cm^{-1} (Fig. 5) which is typically attributed to the Raman peak position of bulk-Ge at room temperature. The intensity of the TO peak is higher for the samples annealed at same temperatures and implanted with 1×10^{17} Ge ions/cm^2 than those of the samples implanted with 5×10^{16} Ge ions/cm^2. The intensity of the band increases with annealing temperature as shown in Figure 6. From these results, we conclude that the size of the nanocrystals increase in samples with higher implantation dose and annealing temperatures as

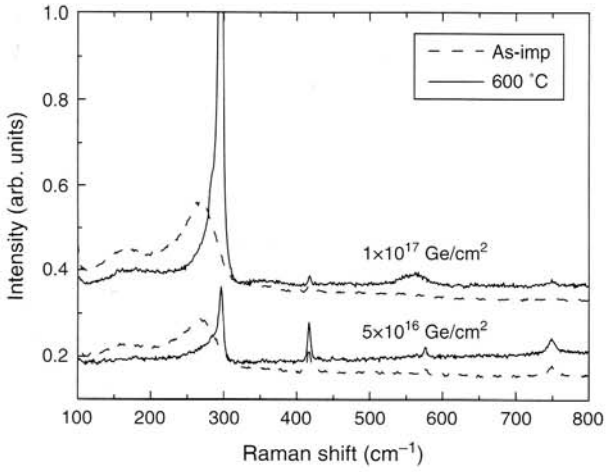

Fig. 5. Raman spectra of the samples implanted with doses of 5×10^{16} Ge ions/cm^2 and 1×10^{17} Ge ions/cm^2 and annealed samples at 600 °C.

expected. On the other hand, Raman signals for the sample implanted with a dose of 5×10^{16} Ge ions/cm^2 and subsequently annealed at 800 °C are increased significantly compared to those annealed at 700 °C. This result is in further agreement with XRD and TEM analysis of the sample annealed at 800 °C, where the size of the nanocrystals is found to increase abruptly.

The shift in the Raman position of Ge nanocrystals with respect to the bulk Ge (~300 cm^{-1}) is dominated by three mechanisms; isotropic composition, phonon confinement, and stress. The natural Ge has 5 different isotopes which generate the Raman signal commonly observed for bulk Ge. In the case of ion implantation, one of the Ge isotopes, which is the one with largest proportion (^{74}Ge) is used for the implantation. This leads to isotropic composition of the Ge within the matrix. A red shift, approximately 3 cm^{-1}, in peak position of the Raman signal of

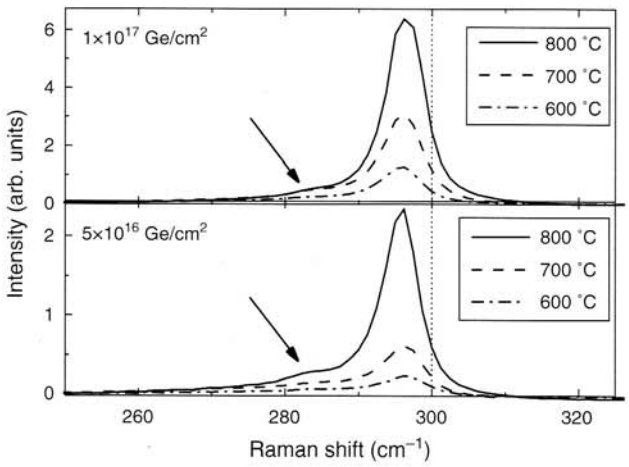

Fig. 6. Raman spectra of the samples implanted with doses of 5×10^{16} Ge ions/cm^2 and 1×10^{17} Ge ions/cm^2 after annealing at temperatures of 600, 700, and 800 °C. The dotted line shows the Raman position of 300 cm^{-1} to guide the eye.

the isotropic ^{74}Ge with respect to natural bulk Ge was estimated.[19] Moreover, it is well-known that the TO band for nanocrystalline Ge shows a broadening in FWHM and a shift to lower wavenumbers due to the phonon confinement effect.[8, 9, 17, 19] According to the standard phonon confinement model using Gaussian weighting function, which is commonly accepted, nanocrystals with diameters of 15 nm and 5 nm undergo down shifts of approximately 1 and 4 cm^{-1}, respectively.[19] When the effects of isotropic composition and phonon confinement on Raman shift are considered, one might expect the Raman position of large and small nanocrystals as ~296 cm^{-1} and ~293 cm^{-1}, respectively. On the other hand, it is known that the stress on nanocrystals can create either down-shift due to tensile stress or up-shift due to compressive stress in Raman spectrum.[8, 9, 17, 19] Extensive stress can cause lattice relaxation with high density of defects in and around Ge nanocrystals. Note that the encapsulated Ge nanocrystals have a lattice constant around 5.65 Å while the surrounding matrix has either lattice constants of 4.758 Å and 12.991 Å for α-Al_2O_3 or 7.90 Å for γ-Al_2O_3. Therefore, it is reasonable to assign the main peak circa 297 cm^{-1} to scattering from large nanocrystals and the bump (highlighted with arrows) at around 284 cm^{-1} to scattering from small nanocrystals. In addition, it is likely that while small nanocrystals are under tensile stress large nanocrystals are under compressive stress. On the other hand, the lack of shift in Raman signal with annealing temperature can be due to the relaxation of large Ge nanocrystals as they can not accommodate the large amount of stress accumulated with increased nanocrystal size.

Recently, several studies have focused on the determination of the stress on Ge nanocrystals formed in SiO_2 matrix using Raman spectroscopy.[9, 17, 19] The calculation is more complicated in the case of sapphire matrix due to possible coexistence of several phases. However, a qualitative analysis can be conducted. The Raman signal of Ge TO band for measured samples does not exhibit a clear shift with the annealing temperature. The lack of shift in the Raman signal can be due both the cancellation of the shifts due to the stress and phonon confinement effect and/or the effect of the relaxation. The defects, produced during the relaxation, can act as a nonradiative transition centers quenching the light emission from nanocrystals.

4. CONCLUSIONS

Formation of Ge nanocrystals in Al_2O_3 matrix by ion implantation at annealing temperatures as low as 500 °C was demonstrated by using various diagnostic techniques. It was shown that Ge nanocrystals with mean sizes of 15 nm and 4 nm were formed in regions near the projected range of implanted ions and underneath this region, respectively. The matrix which was amorphized during the implantation transformed into transition aluminas, probably gamma phase, after the annealing process. The mismatch between transition aluminas and α-Al_2O_3 creates huge stress which forms large amount of defects in the matrix. It seems that large nanocrystals are under compressive stress while small nanocrystals are under tensile stress.

Acknowledgments: This work has been partially supported by the European Commission through the FP6 project called SEMINANO under the contract NMP4-CT-2004-505285.

References and Notes

1. L. Pavesi and D. J. Lockwood (eds.), Silicon Photonics, Topics in Applied Physics Series, Springer-Verlag, Berlin **(2004)**, Vol. 94.
2. R. J. Walters, G. I. Bourianoff, and H. A. Atwater, *Nat. Mater.* 4, 143 **(2005)**.
3. W. Skorupa, L. Rebohle, and T. Gebel, *Appl. Phys. A* 76, 1049 **(2003)**.
4. C. Busseret, S. Ferraton, L. Montes, and J. Zimmermann, *IEEE Trans. Electron Devices* 53, 14 **(2006)**.
5. A. V. Kolobov, S. Q. Wei, W. S. Yan, H. Oyanagi, Y. Maeda, and K. Tanaka, *Phys. Rev. B* 67, 195314 **(2003)**.
6. E. S. Marstein, A. E. Gunnas, U. Serincan, R. Turan, A. Olsen, and T. G. Finstad, *Surface And Coatings Technology* 158, 544 **(2002)**.
7. K. S. Min, K. V. Shcheglov, C. M. Yang, H. Atwater, M. L. Brongersma, and A. Polman, *Appl. Phys. Lett.* 68, 2511 **(1996)**.
8. G. Kartopu, S. C. Bayliss, R. E. Hummel, and Y. Ekinci, *J. Appl. Phys.* 95, 3466 **(2004)**.
9. I. E. Tyschenko, A. B. Talochkin, A. G. Cherkov, K. S. Zhuravlev, and R. A. Yankov, *Solid State Commun.* 129, 63 **(2004)**.
10. Y. Zhu and P. P. Ong, *J. Phys.: Condens. Matter* 13, 4075 **(2001)**.
11. W. M. de Azevedo, E. F. Da Silva, Jr., E. A. De vasconcelos, and H. Boudinov, *Microelectronic J.* 36, 992 **(2005)**.
12. S. Kim, S. H. Choi, C. J. Park, H. Y. Cho, and R. G. Elliman, *J. Korean Phys. Soc.* 45, S501 **(2004)**.
13. Q. Xu, I. D. Sharp, C. Y. Liao, D. O. Yi, J. W. Ager III, J. W. Beeman, K. M. Yu, D. C. Chrzan, and E. E. Haller, *Mater. Res. Soc. Symp. Proc.* 880E, BB5.22.1 **(2004)**.
14. J. F. Ziegler, J. P. Biersack, and U. Littmark, The Stopping and Range of Ions in Solids, Pergamon, New York **(1985)**.
15. For an extensive study on Transition aluminas, see: P. S. Santos, H. S. Santos, and S. P. Toledo, *Mater. Research* 3, 104 **(2000)**. Although Al_2O_3 has many transition phases formed at different temperatures and environmental conditions. γ-Al_2O_3 is the most favorable structure at our target temperatures of 600–800 °C.
16. H. P. Klug and L. E. Alexander, X-Ray Diffraction Procedures, Wiley, New York **(1974)**.
17. S. Yerci, U. Serincan, I. Dogan, S. Tokay, M. Genisel, A. Aydinli, and R. Turan, *J. Appl. Phys.* 100, 074301 **(2006)**.
18. I. D. Desnica-Frankovic, K. Furic, U. V. Desnica, M. C. Ridgway, and C. J. Glover, *Nucl. Instr. and Meth. Phys. Res. B* 178, 192 **(2001)**.
19. A. Welner, V. Pillard, C. Bonafos, H. Coffin, A. Claverie, B. Schmidt, and K. H. Heinig, *J. Appl. Phys.* 94, 5639 **(2003)**.

Received: 11 August 2006. Revised/Accepted: 11 February 2007.